*Inorg. Chem.* **2006**, *45*, 6661–6665


# Hydrothermal Synthesis of Rare-Earth Fluoride Nanocrystals

**Xun Wang,* Jing Zhuang, Qing Peng, and Yadong Li***

*Department of Chemistry, Tsinghua University, Beijing 100084, P. R. China*

Received September 30, 2005

In this paper, a hydrothermal synthetic route has been developed to prepare a class of rare-earth fluoride nanocrystals, which have shown gradual changes in growth modes with decreasing ionic radii and may serve as a model system for studying the underlying principle in the controlled growth of rare-earth nanocrystals. Furthermore, we demonstrate the functionalization of these nanocrystals by means of doping, which have shown visible-to-the-naked-eye green up-conversion emissions and may find application in biological labeling fields.

## Introduction

Rare-earth nanocrystals with controllable shapes and sizes have received intense research attention during the past few years[1−12] because of their potential applications in optics,[1−3] optoelectronics, biological labeling,[4,5] catalysis fields,[6] etc. It is expected that with reduced dimensionalities, the movement of electrons and photons in rare-earth nanocrystals would be confined in two and/or all directions and then lead to enhanced optical and magnetic properties in a manner similar to that of typical systems such as II−VI semiconductor nanocrystals.[13−17] This is particularly important for the exploration of new research and application fields on the basis of the novel properties of rare-earth nanocrystals. However, there still remains much to be carefully addressed in the rare-earth nanocrystal system, especially for the general principle in shape and size control, which may provide possibilities for systematically investigating the size- and shape-dependent properties on the nanoscale. Here, we present the controlled synthesis of a class of rare-earth fluoride nanocrystals, which have shown gradual changes in growth modes with decreasing ionic radii and may serve as a model system for studying the underlying principle in the controlled growth of rare-earth nanocrystals.

To get high quality nanocrystals, one usually needs to engineer the surface properties and in some cases modulate the growth dynamics of nanocrystals. Until now, many important compounds have been processed into monodisperse nanocrystals via metal−organic or various solution-based synthetic routes, including II−VI,[13−17] noble metals,[18] transitional-metal elements,[19] magnetic $MFe_2O_4$,[20] various oxide nanocrystals,[21] etc. All these successes largely depend on the discovery of a certain new reaction system proven as being effective in confining the growth of a specific

* To whom correspondence should be addressed. E-mail: wangxun@mail.tsinghua.edu.cn (X.W.); ydli@mail.tsinghua.edu.cn (Y.L.).

(1) Riwotzki, K.; Meyssamy, H.; Schnablegger, H.; Kornowski, A.; Haase, M. *Angew. Chem., Int. Ed.* **2001**, *40*, 573−576.
(2) Heer, S.; Lehmann, O.; Haase, M.; Gudel, H. U. *Angew. Chem., Int. Ed.* **2003**, *42*, 3179−3182.
(3) Stouwdam, J. W.; van Veggel, F. C. J. M. *Nano Lett.* **2002**, *2*, 733−737.
(4) Yi, G. S.; Lu, H. C.; Zhao, S. Y.; Yue, G.; Yang, W. J.; Chen, D. P.; Guo, L. H. *Nano Lett.* **2004**, *4*, 2191−2196. Yi, G. S.; Chow, G. M. *J. Mater. Chem.* **2005**, *15*, 4460−4464.
(5) Wang, L. Y.; Yan, R. X.; Huo, Z. Y.; Wang, L.; Zeng, J. H.; Bao, J.; Wu, H. K.; Wang, X.; Peng, Q.; Li, Y. D. *Angew. Chem., Int. Ed.* **2005**, *44*, 6054−6057. Zeng, J. H.; Su, J.; Li, Z. H.; Yan, R. X.; Li, Y. D. *Adv. Mater.* 2005, 17, 2119. Yan, R. X.; Li, Y. D. *Adv. Func. Mater.* **2005**, *15*, 763−770.
(6) Zhou, K. B.; Wang, X.; Sun, X. M.; Peng, Q.; Li, Y. D. *J. Catal.* **2005**, *229*, 206−212.
(7) Wang, X.; Li, Y. D. *Angew. Chem., Int. Ed.* **2002**, *41*, 4790−4793.
(8) Wang, X.; Sun, X. M.; Yu, D. P.; Zou, B. S.; Li, Y. D. *Adv. Mater.* **2003**, *15*, 1442−1445.
(9) Wang, X.; Li, Y. D. *Angew. Chem., Int. Ed.* **2003**, *42*, 3497−3500.
(10) (a) Yan, R. X.; Sun, X. M.; Wang, X.; Peng, Q.; Li, Y. D. *Chem.−Eur. J.* **2005**, 11, 2183-2195. (b) Fang, Y. P.; Xu, A. W.; Song, R. Q.; Zhang, H. X.; You, L. P.; Yu, J. C.; Liu, H. Q. *J. Am. Chem. Soc.* **2003**, *125*, 16025−16034.
(11) Zhang, Y. W.; Sun, X.; Si, R.; You, L. P.; Yan, C. H. *J. Am. Chem. Soc.* **2005**, *127*, 3260−3261.
(12) Si, R.; Zhang, Y. W.; You, L. P.; Yan, C. H. *Angew. Chem., Int. Ed.* **2005**, *44*, 3256−3260.
(13) Murray, C. B.; Norris, D. J.; Bawendi, M. G. *J. Am. Chem. Soc.* **1993**, *115*, 8706−8715.
(14) Peng, X. G.; Manna, L.; Yang, W. D.; Wickham, J.; Scher, E.; Kadavanich, A.; Alivisatos, A. P. *Nature* **2000**, *404*, 59−61.
(15) Murray, C. B.; Kagan, C. R.; Bawendi, M. G. *Science* **1995**, *270*, 1335−1338.
(16) Chan, W. C. W.; Nie, S. M. *Science* **1998**, *281*, 2016−2018.
(17) Bruchez, M.; Moronne, M.; Gin, P.; Weiss, S.; Alivisatos, A. P. *Science* **1998**, *281*, 2013−2016.
(18) Sun, Y. G.; Xia, Y. N. *Science* **2002**, *298*, 2176−2179.
(19) Sun, S. H.; Murray, C. B.; Weller, D.; Folks, L.; Moser, A. *Science* **2000**, *287*, 1989−1992.
(20) Sun, S. H.; Zeng, H.; Robinson, D. B.; Raoux, S.; Rice, P. M.; Wang, S. X.; Li, G. X. *J. Am. Chem. Soc.* **2004**, *126*, 273−279.
(21) Park, J.; An, H. J.; Hwang, Y. S.; Park, J. G.; Noh, H. J.; Kim, J. Y.; Park, J. H.; Hwang, N. M.; Hyeon, T. *Nat. Mater.* **2004**, *3*, 891−895.

10.1021/ic051683s CCC: $33.50 
Published on Web 07/19/2006

compound. Because of the complexity of the crystal structures and compositions, it is still a difficult challenge to clearly define the interaction between the protecting reagents and the nanocrystals, which may be the key in developing a general method for the controlled growth of nearly monodisperse nanocrystals. Rare-earth compounds represent a class of interesting materials. All the lanthanide atoms have close and gradually changing ionic radii, and as a result, the physical and chemical properties change correspondingly. Previous studies on the lanthanide hydroxide nanowires/nanorods[7] and nanotubes[8] as well as lanthanide orthophosphate nanocrystals[1,2] and nanowires[10] indicate that controlled growth of lanthanide compounds usually leads to gradual changes in morphologies with decreasing ionic radii and the subsequent altering of the crystal structures. If we could develop a general method for preparing nearly monodisperse lanthanide compounds nanocrystals, it would be possible to investigate the influences of gradual changes in ionic radii and crystal structures on the crystal growth on the nanoscale. Especially, it would be possible to investigate the interaction between complexation reagents and the nanocrystals systematically, and thus bring us a clearer understanding on the controlled synthesis of rare-earth nanocrystals. All the synthesis procedures were based on an LSS procedure for preparing various nanocrystals,[22] the success of which depends on the effective complexation of linoleate on the surfaces of nanocrystals in a water−ethanol mixed-solution system. Here, we have expanded this method to the synthesis of a whole group of rare-earth fluoride nanocrystals.

## Experimental Section

**Synthesis of Rare-Earth Fluoride Nanocrystals.** In a typical synthesis, 1.6 g of sodium linoleate, 4 mL of linoleate acid, and 16 mL of ethanol were mixed together under agitation to form a homogeneous solution; aqueous solutions of $Ln(NO_3)_3$ (0.5 g/7.5 mL distilled water; Ln = La, Ce, Pr, Nd, Sm, Eu, Gd, Th, Dy, Ho, Er, Tm, Yb, and Y) and NaF/or $NH_4HF_2$ (0.2 g/7.5 mL distilled water) were then added. The mixture was agitated for about 5 min and then transferred to a 40 mL autoclave, sealed, and hydrothermally treated at a designed temperature of 100−200 °C for about 8−10 h. The system was then allowed to cool to room temperature, and the products were deposited at the bottom of the vessel. The final products can be well-dispersed in a nonpolar solvent and then deposited in a polar solvent. Cyclohexane was used to collect the products deposited in the vessel. The products were deposited by adding ethanol to the sample-containing cyclohexane solution. The solution was then centrifuged to obtain the powder samples. The pure powders can be obtained by purifying the samples with ethanol several times to remove oleic acid, sodium linoleate, and other remnants.

Following this procedure, $LnF_3$ (Ln = La, Ce, Pr, Nd, Sm, Eu, Gd, Th, Dy, Ho, Er, and Tm), $NaYF_4$, and $NaYb_2F_7$ nanocrystals could be rationally obtained. To get $YF_3$ and $YbF_3$, we adopted to replace sodium linoleate with 0.5 g of octadecylamine and used $NH_4HF_2$ instead of NaF.

**Characterization.** The obtained sample was characterized on a Bruker D8-Advance X-ray powder diffractometer with Cu Kα radiation ($\lambda$ = 1.5418 Å). The size and morphology of the IF nanoparticles were determined at 200 kV by a Hitachi H-800 transmission electron microscope (TEM) and a JEOL JEM-2010F high-resolution transmission electron microscope. Samples were prepared by placing a drop of a dilute cyclohexane dispersion of nanocrystals on the surface of a copper grid. Fluorescence spectra were recorded with a Hitachi F-4500 fluorescence spectrophotometer. Up-conversion fluorescence spectra were obtained with the LS-50B fluorescence spectrophotometer (Perkin−Elmer Corp., Forster City, CA) with an external 0−800 mW adjustable laser (980 nm, Beijing Hi-Tech Optoelectronic Co., China) as the excitation source, instead of the Xenon source in the spectrophotometer, and with an optic fiber accessory.

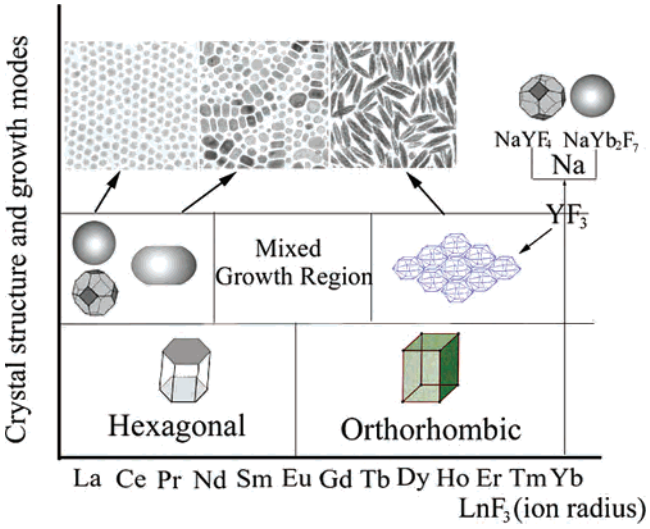


**Figure 1.** Phase diagram and growth modes of $LnF_3$ nanocrystals.

## Results and Discussion

Crystal structure has been proven as being one of the most important factors that will influence the growth behavior of nanocrystals, so our emphasis was placed on the direct correlation between the crystal structure of the rare-earth fluoride compounds and their morphologies. Under identical synthetic conditions, two different types of crystal structures of the as-obtained $LnF_3$ products have been identified by means of XRD analysis. XRD data of the obtained hexagonal fluorides (from La to Eu) and orthorhombic fluorides (from Gd to Yb and Y) are shown in Figures 1 and 2. As examples, all the peaks of the XRD patterns for each sample in Figure 2A can be readily indexed to a pure hexagonal phase of $LaF_3$ and $PrF_3$. Because of the small size of the nanocrystals and the overlapping of the diffraction peaks, the pattern is apparently broadened. All diffraction peaks shown in Figure 2B are characteristic of a pure orthorhombic phase of $LnF_3$ (Dy, Ho, Er, and Y). Because Y has a close ion radius with Yb, $YF_3$ adopted an orthorhombic phase as well. It is also found that Na can be incorporated into the framework of Ln−F and result in face-centered cubic $NaYF_4$ and orthorhombic $NaYb_2F_7$ (Figure 2C) in the case of Y and Yb when NaF was used as the $F^-$ source. All these experimental results have drawn the outline of the phase diagram of the Ln−F system (Figure 1), which may serve as a basis for the

(22) Wang, X.; Zhuang, J.; Peng, Q.; Li, Y. D. *Nature* **2005**, *437*, 121−124.

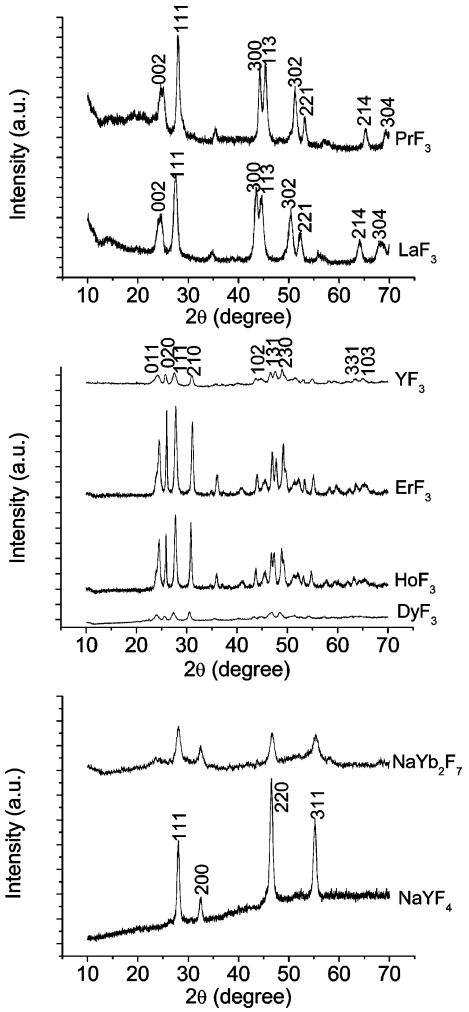


**Figure 2.** XRD patterns of $LnF_3$ (at a temperature condition of 120 °C).

investigation of the growth of rare-earth fluoride nanocrystals under the adopted experimental conditions.

Similar to in the synthesis of lanthanide hydroxides and orthophosphate nanowires/nanorods, nanocrystals show a gradual change in morphology during their synthesis. But our studies show that the growth modes are more complicated. Although the crystals structures of $LnF_3$ adopt only hexagonal and orthorhombic type, the whole growth region can be classified into three distinct regions of La−Nd, Sm−Gd, and Tb−Yb. And with the incorporation of Na into the framework of F−Ln, the forth mode exists for these compounds (Figure 1).

In the region of La−Nd, as shown in Figure 3, all the samples on the TEM grid show morphologies of well-dispersed nearly round-shaped nanocrystals or partly elongated nanoparticles. $LaF_3$ nanocrystals with narrower size distributions self-assemble into close-packed 2-D arrays on the TEM grids with the evaporation of solvents (panels B and H of Figure 3). HRTEM characterization shows that the nanocrystals are single crystalline (Figure 3I). Different from the reported $LaF_3$ triangular nanoplates,[11] the as-obtained $LaF_3$ nanocrystals show nearly round morphologies, which may mean that no growth direction is dominant during the growth of these nanocrystals. For the $PrF_3$ nanocrystals, TEM characterization proves that they are composed of a mixture of nearly round-shaped nanocrystals and elongated nanoparticles (Figure 3E), and the elongated particles partly self-assemble into arrays. Electron patterns (Figure 3F) taken from the $PrF_3$ nanocrystals reveal that they are crystalline and can be indexed as the (002), (111), (300), and (302) planes of hexagonal $PrF_3$. All the nanocrystals are quite dispersed, indicating that the current system is rather efficient in preventing the nanocrystals from agglomeration. However, the morphologies of the nanocrystals are slightly different. Because all these fluorides share the same crystal structure and similar atom distribution in spaces, it might be reasonable to imagine that the complexation of linoleate molecular is

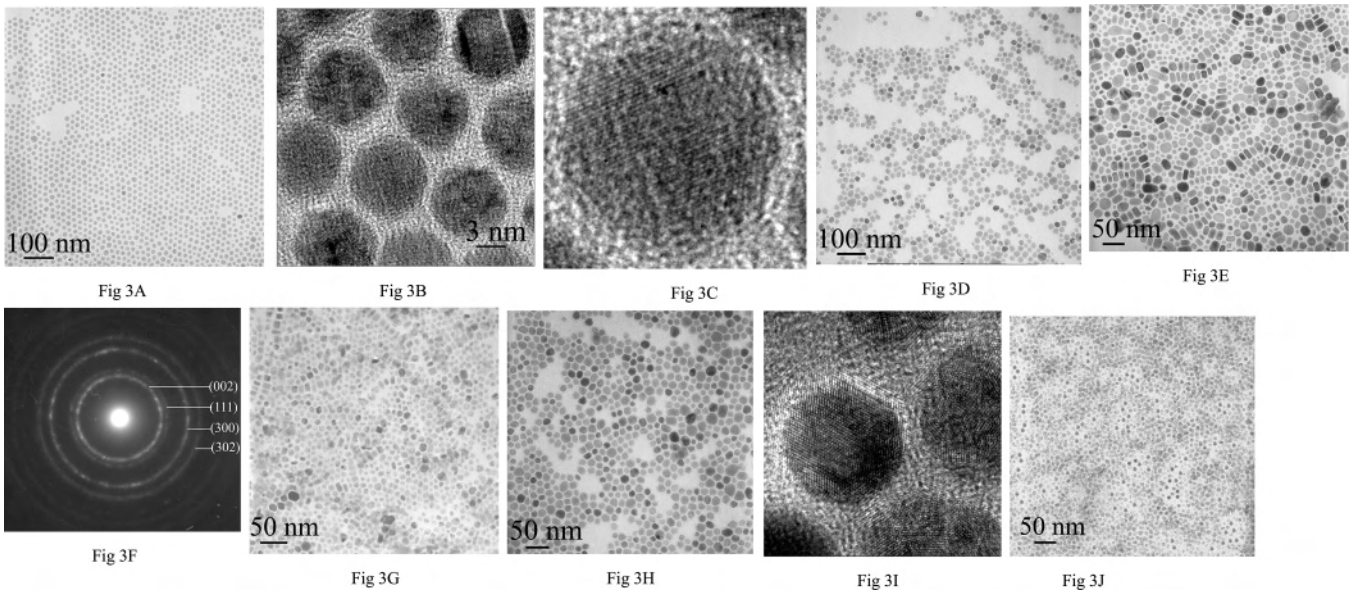


**Figure 3.** TEM images of (A) $NaYF_4$ nanocrystals (120 °C); (B, C) HRTEM images of $NaYF_4$ nanocrystals; (D) $CeF_3$ nanocrystals (120 °C); (E) $PrF_3$ nanocrystals (120 °C); (F) Electron-diffraction patterns taken from $PrF_3$ nanocrystals; (G) $NdF_3$ nanocrystals (120 °C); (H) $LaF_3$ nanocrystals (120 °C); (I) HRTEM images taken from individual $LaF_3$ nanocrystals; and (J) $NaYb_2F_7$ nanocrystals (120 °C).

quite sensitive to the slight changes of the distance between Ln and F atoms. This assumption was confirmed when this system was expanded to Sm, Eu, and Gd.

As mentioned above, the fluoride will follow an orthorhombic crystal structure for $GdF_3$ and compounds after Gd. For Sm and Eu, the structure and atom distribution still follow the $LaF_3$ type hexagonal structures. But our experiments show that, unlike the synthesis of nanowires/nanorods, the confined growth of fluoride nanocrystals cannot be easily expanded to the whole group of compounds. All the efforts to prepare $SmF_3$, $EuF_3$, and $GdF_3$ under identical conditions have failed. And TEM characterizations show that the samples are mainly composed of irregular particles in micrometer sizes. This means that under identical experimental conditions, the absorption and/or complexation of linoleate molecules are not as effective as in the La, Ce, Pr, and Nd fluorides, although the radius of the lanthanide atoms shrink only a little.

As can be seen from Figure 1 and the XRD data of $LnF_3$ (Ln = La−Eu, Figure 2), the crystal structures of $LnF_3$ all follow a hexagonal pattern, and the *a*:*c* ratios have nearly the same value of 0.973−0.978. On the basis of previous studies on the controlled synthesis of 1-D nanostructures, crystals with a preferential axis might prefer to grow along a certain direction and have the morphologies of nanowires or nanorods; such examples can be found in the synthesis of CdSe[14] and ZnO nanorods[23] as well as lanthanide hydroxide nanowires.[7] Under the current experimental conditions, the growth of hexagonal $LaF_3$ and $CeF_3$ nanocrystals have been passivated in nearly all directions and thus have morphologies of nearly round and truncated cubic shape (panels D and H of Figure 3), whereas the $PrF_3$ crystals (Figure 3E) have shown elongated morphologies to some extent due to the preferential axis. Dispersion and agglomeration may be the decisive factors that will determine the growth of nanocrystals. Usually, there exists a balance between the dispersion and agglomeration for the nanocrystals. Factors that favor the dispersion of nanocrystals include brown movement, the electrostatic repulsion due to the electronic properties of the surfaces, and the steric effects of foreign molecules complexed on the nanocrystals. In current studies, effective complexation of linoleate molecules on the outer surfaces of the fluoride nanocrystals is apparently the decisive factor. It is reasonable to imagine that, with the changing of central atoms and crystal structures, the complexation state on different crystal surfaces of the nanocrystals changes slightly, which leads to different growth modes. For $SmF_3$, $EuF_3$, and $GdF_3$, the complexation of linoleate molecular on nearly all the crystal planes are not effective, so the monomers can overgrow on the nanocrystals and lead to irregular micrometer-sized crystals.

Things become quite different when we try to grow $LnF_3$ nanocrystals after the Gd. It is interesting to find that the samples are composed of uniform ricelike nanocrystals (Figure 4). Because Y has an ionic radius similar to that of

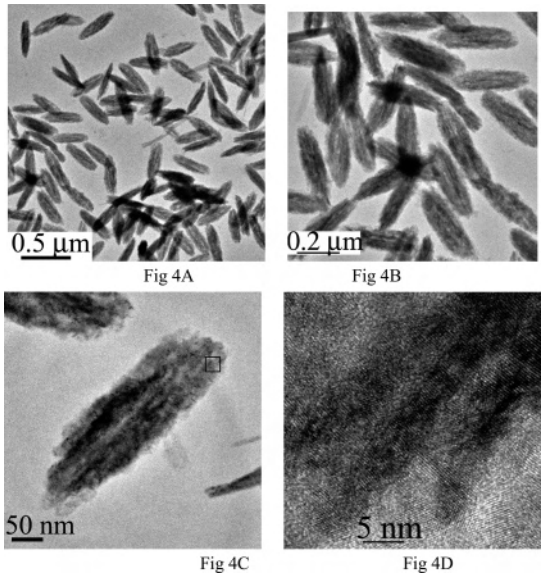


**Figure 4.** TEM images of (A−D) $YF_3$ nanocrystals (120 °C) with different magnifications.

Yb, $YF_3$ could be prepared as an orthorhombic structure. All the nanocrystals are rather uniform with a typical aspect ratio of 3−4. Peng et al. have reported the synthesis of ricelike CdSe nanocrystals by tuning the growth dynamics of the CdSe reaction system.[24] However, the current samples are quite different. TEM images of higher magnification show that the samples are indeed composed of short nanorods (panels C and D of Figure 4). These indicate that the nanocrystals are in a special form of agglomeration. Take $YF_3$ as an example; Figure 4D shows the HRTEM images of $YF_3$ ricelike nanocrystals, from which the aligned nanorods can be clearly discerned. The interlayer spacing can be calculated to be about 0.311 nm, corresponding to the (111) planes of orthorhombic $YF_3$. We have attributed the synthesis of $LaF_3$ nanocrystals to the effective absorption/complexation of linoleate molecules on the outer surfaces. In this case, we believe that the nanocrystals in their initial formation stage can be covered only in certain crystal planes, which result in more reactive (111) planes and the tendency to grow along ⟨111⟩ directions. It is apparent that the complexation of linoleate molecules on the crystal planes is not as effective as that of fluorides such as La−Nd.

Na could be incorporated into the matrix of Ln−F and form cubic $NaYF_4$ and orthorhombic $NaYb_2F_7$ in the cases of Y and Yb, respectively. TEM characterizations show that all the samples dispersed on the TEM grids show well-dispersed nearly round or truncated cubic-shaped nanocrystals (Figure 3A−C and J). Compared with the aqueous synthetic routes,[4,5] the as-obtained $NaYF_4$ nanocrystals are more dispersed and uniform in size because of the effective absorption of linoleic acid on the surface. Because the adopted linoleic acids are anion surfactants, the favorable absorption sites should be the central metal cations. Considering that $YF_3$ and $NaYF_4$ share the same central metal cations of Y, whereas they are different in the atom distribution of Y and F and the incorporation of Na, it is

(23) Huang, M. H.; Mao, S.; Feick, H.; Yan, H. Q.; Wu, Y. Y.; Kind, H.; Weber, E.; Russo, R.; Yang, P. D. *Science* **2001**, *292*, 1897−1899.

(24) Peng, Z. A.; Peng, X. G. *J. Am. Chem. Soc.* **2002**, *124*, 3343−3353.

clear that the incorporation of Na into the framework of Y−F may increase the complexation sites of linoleate on the surface of the $NaYF_4$. Another possible reason for this growth behavior may be the inherent face-centered cubic crystal structure of $NaYF_4$. A general sequence of surface energies for crystals with face-centered cubic structures is $\gamma\{111\} < \gamma\{100\} < \gamma\{110\}$. On the basis of the surface free-energy minimization principle, we expect the equilibrium morphology of $NaYF_4$ to be truncated cubic. However, considering that the orthorhombic $NaYb_2F_7$ has shown a morphology similar to that of $NaYF_4$, it is most probable that the incorporation of Na into the framework of Ln−F greatly increases the complexation sites for the anion surfactants in all the crystal planes so that the growth is passivated in all directions. In the fourth growth mode, the decisive factors for the growth behavior would be the increasing complexation sites induced by the incorporation of Na ions.

Many experimental parameters may influence the growth of materials, and the inherent and most important one would be the crystal structures.[26] Current studies further indicate that under hydrothermal conditions, the complexation of surfactants on the crystal surfaces are rather sensitive to the slight changes in atom distributions for compounds sharing the same space group and crystal structures, which may be suggestive of the designed synthesis of other inorganic nanocrystals.

Rare-earth compounds are distinguished for their luminescence properties, and different doping modes may lead to quite different emission behavior, which are appealing to applications such as biological labeling and optics.[25] Especially nanometer-sized up-conversion phosphors with uniform size and high luminescence efficiency are desirable as sensitive biological labeling material for the detection of biomolecules such as DNA, RNA, or proteins.[4,5] In the past years, several successful examples have been demonstrated for the synthesis of rare-earth compound nanocrystals with up-conversion properties.[4,5,25] Our method has also been shown to be effective in producing doped nanocrystals with up-conversion properties. For example, the most frequently used up-conversion ions, $Er^{3+}$, were adopted in combination with $Yb^{3+}$ as a sensitizer to induce up-conversion in $NaYF_4$ nanoparticles. And when excited by the 980 nm laser, the cyclohexane solution of $NaYF_4$ nanocrystals has shown strong green up-conversion emissions (Figure 5). The green light emission bands centered at 526 and 552 nm correspond to $2H_{11/2}$ and $4S_{3/2}$ transitions to the $4I_{15/2}$ ground state, respectively. The red-light emission band centered on 663 nm corresponds to the $4F_{9/2}$ to $4I_{15/2}$ transitions. These results substantiate the successful doping of $Er^{3+}/Yb^{3+}$ into $NaYF_4$ nanocrystals and make these nanocrystals appealing to wide applications.

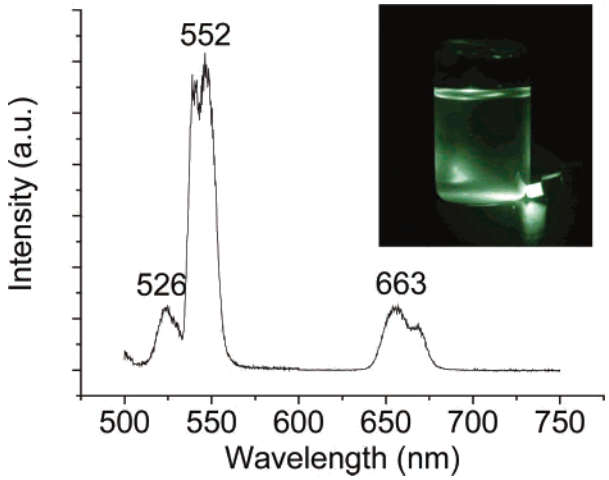


**Figure 5.** Visible-to-the-naked-eye green up-conversion emissions (inset) and spectra of Yb/Er-co-doped $NaYF_4$ nanocrystals (Y:Yb:Er = 100:20:2), excited with a 980 nm laser.

In this paper, we have demonstrated the controlled synthesis of rare earth fluoride nanocrystals through a facile hydrothermal synthetic way. With decreasing ionic radii, the growth modes of rare-earth fluorides changes significantly, which may provide a model system for investigating the growth of inorganic nanocrystals and thus bring more opportunities to the nanocrystal fields of research and applications.

**Acknowledgment.** This work was supported by NSFC (20501013, 50372030, 90406003), the Foundation for the Author of National Excellent Doctoral Dissertation of P. R. China, and the State Key Project of Fundamental Research for Nanomaterials and Nanostructures (2003CB716901).

IC051683S

(25) Heer, S.; Köpme, K.; Güdel, H. U.; Haase, M. *Adv. Mater.* **2004**, *16*, 2102−2105.
(26) Wang, X.; Li, Y. D. *Pure Appl. Chem.* **2006**, *78*, 45−64.